Journal of Alloys and Compounds 509 (2011) 3190–3196

Contents lists available at ScienceDirect

Journal of Alloys and Compounds

journal homepage: www.elsevier.com/locate/jallcom

Influence of titanium and chromium addition on the microstructure and mechanical properties of squeeze cast Mg–6Al alloy

S. Can Kurnaz*, Hüseyin Sevik, Sehzat Açıkgöz, Ahmet Özel

Sakarya University, Faculty of Engineering, Department of Metallurgical and Materials Engineering, Adapazarı, 54187, Turkey

ARTICLE INFO

Article history:
Received 6 September 2010
Received in revised form 7 December 2010
Accepted 8 December 2010
Available online 15 December 2010

Keywords:
Mg–6Al alloy
Microstructure
Mechanical properties
Wear

ABSTRACT

In this study, the effect of titanium and chromium (0, 0.1, 0.2, 0.3, and 0.4 wt%) on the microstructure, mechanical and wear properties of a magnesium-based alloy (Mg–Al 6 wt%) were investigated. The alloys were produced under a controlled atmosphere by a squeeze-casting process. The results show that the addition of Ti element modified the structure and decreased the grain size. A similar trend is also observed in the alloys containing Cr. The results of hardness, tensile and impact testing indicate that the hardness, tensile and impact strength of Mg–6Al alloy increased by adding Ti up to 0.2 wt% and then is relatively constant with increasing Ti. A similar result is also observed in the alloys containing Cr. The wear rate of Mg–6Al alloy decreased with increasing alloying elements up to 0.2 wt%. Then the wear rate is relatively constant with the addition of more alloying elements. While the friction coefficient value of Mg–6Al alloy gradually increased with increasing Cr, the friction coefficient value of Mg–6Al alloy decreased with increasing Ti up to 0.2 wt%. Then the friction coefficient value is constant with increasing Ti.

1. Introduction

One of the most important things for the world in the next century is to decrease the fuel costs for vehicles and to further the reduction of emissions to lower our growing environmental impact. The utilization of magnesium and its alloys in the automotive industry has therefore significantly increased in past few years. However, only a few magnesium alloys especially produced by pressure die-casting are used because of having lower mechanical properties and wear resistance than aluminum alloys [1–7]. In general, magnesium alloys are based on Mg–Al systems which are relatively cheap compared with other magnesium alloys available. It is well known, Al containing Mg alloys include the β-$Mg_{17}Al_{12}$ compound that detrimentally influences the mechanical properties such as tensile strength and impact resistance [2,9–12]. One of the most efficient ways to decrease the detrimental effect of the β-$Mg_{17}Al_{12}$ phase on the mechanical properties is to addition third alloying element [13–16].

Besides, wear properties are also significant when magnesium alloys are to be applied for critical automobile applications. However, few studies on wear properties of magnesium alloys have been reported [4–7]. Hence, their wear properties are not understood much in detail compared to other structural components. These studies were observed that the reduction of grain size of magnesium alloys is positively affected for their wear properties [4,8]. The grain refinement effect of alloying elements can be explained in terms of the growth restriction factor (GRF) value, and Ti has a very pronounced grain-refining effect on Mg–Al based alloys even at very low concentrations [17–19], while there is no information reported for Cr-containing Mg–Al alloys. What is more, the wear behavior of magnesium alloys can be affected by the hardness of the base alloys under constant sliding and dry loading conditions [6,20]. The aim of the present study is to investigate the mechanical and wear properties and the microstructure of magnesium–aluminum-based alloy Mg–6Al alloyed with Ti and Cr.

2. Experimental details

The alloys, with compositions listed in Table 1, were prepared using commercially pure magnesium and aluminum in a steel crucible with an electric resistance furnace protected by CO_2-1%SF_6. Chromium and titanium were added as Al–40Cr and Al–6Ti master alloy. The casting parameters were as follows: the melt of matrix alloy was held at a 720 °C casting temperature for 20 min, a 120 °C mold temperature and a 100 MPa filling pressure.

Metallographic samples were first cut on a wire erosion machine. Grinding was performed using silicon carbide (SiC) grinding papers up to 1200 grit. Prior to polishing, the samples were rinsed with ethanol, and then polishing was performed with a 0.05 μm alumina solution. The specimens for optical microscopy (OM) and scanning electron microscopy (SEM) were chemically etched in acetic picric (5 ml acetic acid, 6 g picric acid, 10 ml distilled water, 100 ml ethanol) to show grain boundaries and nital (4 ml nitric acid, 96 ml ethanol) for revealing structure. In addition, the distribution of alloying elements in the structure was verified by using an SEM instrument (JEOL 6060LV) with an energy-dispersive spectrometer (EDS). X-ray diffraction (XRD) analysis was also carried out to identify the phases present in the samples using a Rigaku D-Max 1000 X-ray diffractometer with Cu Kα radia-

* Corresponding author. Tel.: +90 2642955789; fax: +90 2642955549.
E-mail address: ckurnaz@sakarya.edu (S.C. Kurnaz).

0925-8388/$ – see front matter © 2010 Elsevier B.V. All rights reserved.
doi:10.1016/j.jallcom.2010.12.055

Table 1
The chemical composition of the investigated alloys (mass fraction, %).

Alloy no.	Alloy	Al	Ti	Cr	Mg
Alloy 1	Mg–6Al	5.891	–	–	Bal.
Alloy 2	Mg–6Al–0.1Ti	5.818	0.074	–	Bal.
Alloy 3	Mg–6Al–0.2Ti	5.901	0.143	–	Bal.
Alloy 4	Mg–6Al–0.3Ti	5.879	0.261	–	Bal.
Alloy 5	Mg–6Al–0.4Ti	5.809	0.337	–	Bal.
Alloy 6	Mg–6Al–0.1Cr	5.891	–	0.081	Bal.
Alloy 7	Mg–6Al–0.2Cr	5.821	–	0.154	Bal.
Alloy 8	Mg–6Al–0.3Cr	5.875	–	0.253	Bal.
Alloy 9	Mg–6Al–0.4Cr	5.843	–	0.323	Bal.

tion. The grain size measurements were performed by using image analysis software (Clemex).

Brinell hardness tests were carried out on ground and polished samples with a ball diameter of 2.5 mm and an applied load of 31.25 kg. At least 10 impressions were made to determine the mean value of the hardness. Tensile tests were performed using an Instron 3367 universal testing machine at cross head speed of 0.2 mm/s. Each test was repeated five times, and the average values were accepted as the experimental result.

Un-notched impact test samples measured 55 mm × 10 mm × 10 mm were cut on a wire erosion machine and then polished using alumina paste. The testing was carried out using Charpy impact test machine at room temperature and at least three runs were performed. The wear test was performed using a pin-on-disc type apparatus. The test materials in the form of pins of 5 mm diameter and 20 mm length were made to slide against a rotating heat treated DIN 4140 steel disc of 63 in Rockwell (R_c) and diameter 100 mm. Before the wear tests, each specimen was ground up to grade 1200 abrasive paper and polished, making sure that the wear surface was in entire contact with the surface of the steel disk. Before each test, specimen was cleaned with alcohol. Wear tests were carried out under dry sliding conditions under the 10 N load, at sliding speed of 1.2 m s^{-1} and a total sliding distance of about 1 km. Each test was performed with a fresh disk surface and at least three runs were performed. Wear losses were obtained by determining the masses of samples before and after wear tests. An electronic balance having an accuracy level of 0.001 mg was used to measure the weight loss. The specific wear rate of the pins is defined as the weight loss per unit sliding distance.

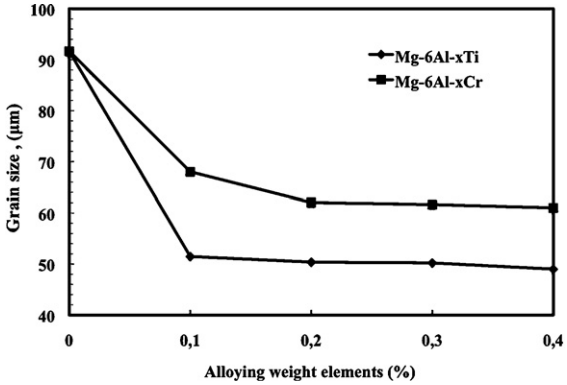

Fig. 1. The effect of alloying elements on grain size of Mg–6Al alloy.

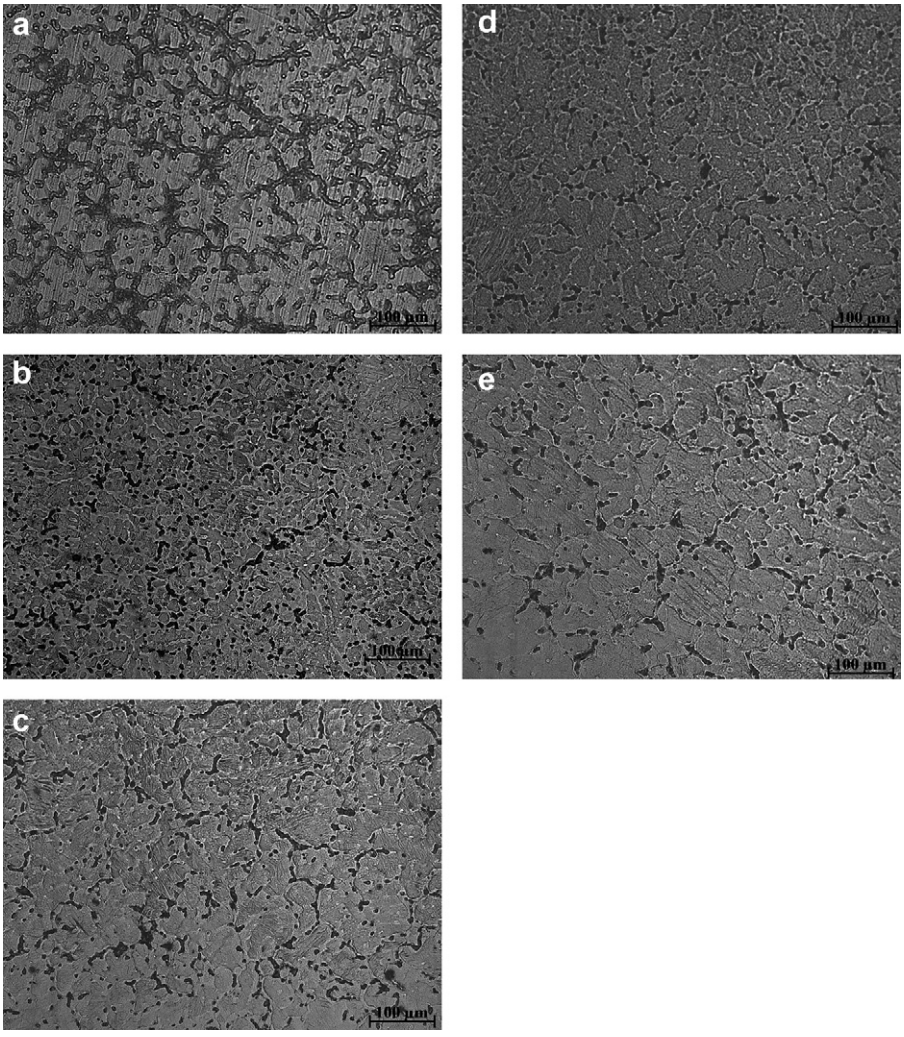

Fig. 2. Optical microstructures of: (a) Mg–6Al, (b) Mg–6Al–0.1Ti, (c) Mg–6Al–0.4Ti, (d) Mg–6Al–0.1Cr, (e) Mg–6Al–0.4Cr alloy.

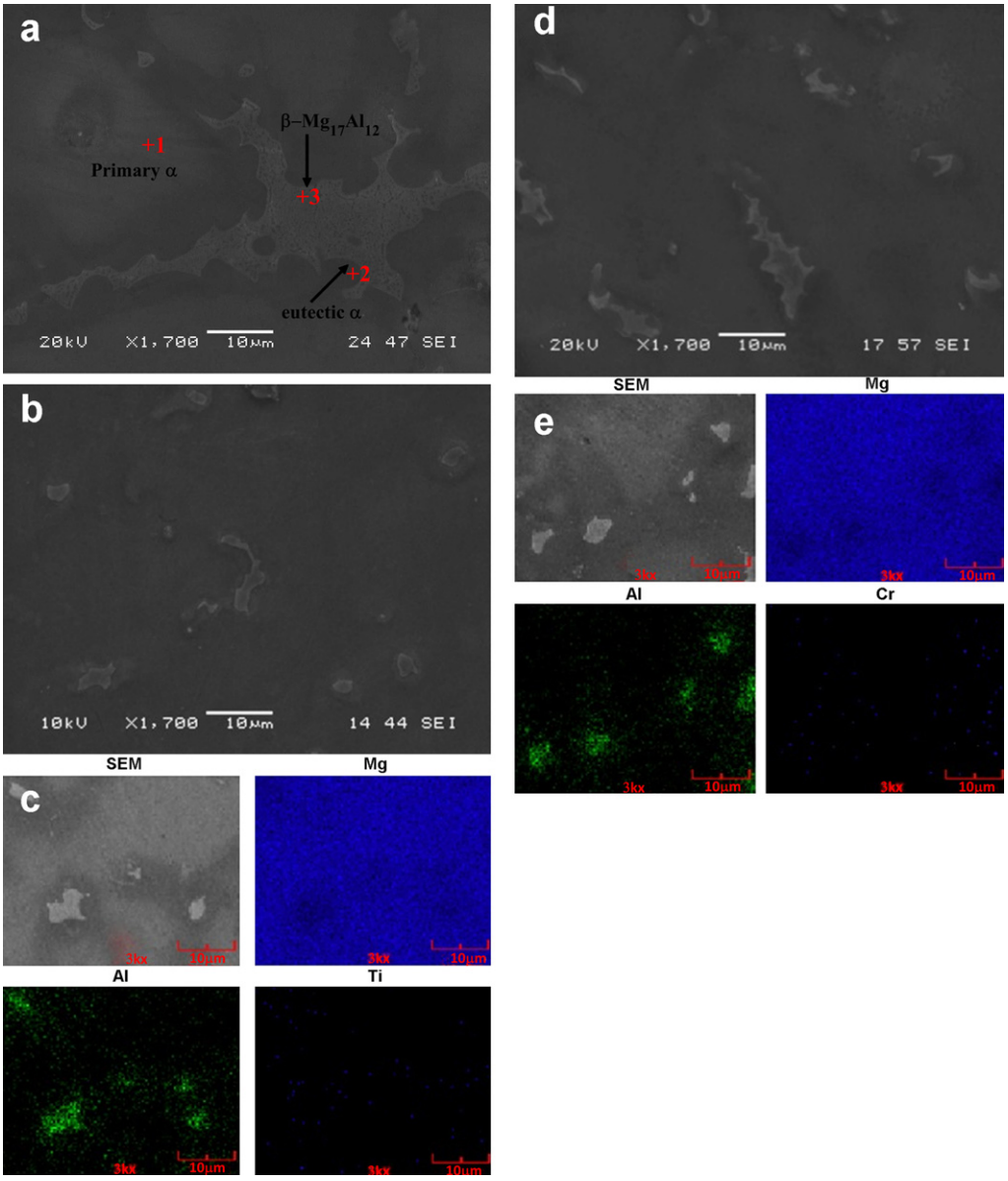

Fig. 3. SEM micrograph showing microstructure and EDS analysis of (a) squeeze cast Mg–6Al, (b) and (c) Mg–6Al–0.4Ti, (d) and (e) Mg–6Al–0.4Cr alloy.

3. Results and discussion

3.1. Microstructure and characterization

Fig. 1 shows the influence of different amounts of alloying elements addition into alloy 1 on the grain size. It obviously shows that the grain size of alloy 1 decreases with increasing quantity of alloying element addition. The grain size of the alloy 1 decreases from 91 to 49 μm when the amount of Ti added increases from 0 to 0,4 wt%, respectively. With addition of Cr, the grain size of alloy 1 decreases from 91 to 61 μm. Several methods are available for grain refining magnesium alloys, however, the mechanisms involved are not understood clearly. A recent study indicates that AZ31, AZ61 and ZA84 alloys can be grain refined by the use of Al–Ti–B type grain refiners. Those master alloys consist of Al_3Ti and TiB_2 particles, in which either the Al_3Ti and TiB_2 or both types of particles act as heterogeneous nucleation sites, like aluminum alloys [21–23]. According to the Al–Ti and Al–Cr binary phase diagrams, the Al–6Ti and Al–40Cr master alloys consist of Al_3Ti and Al_4Cr particles, respectively. In this study, Al_3Ti and Al_4Cr particles dissolve when the master alloys added into molten alloy 1. Therefore, the Ti and Cr are assumed to serve as heterogeneous nuclei of α-Mg.

Optical micrographs of some produced alloys are shown in Fig. 2. As shown in Fig. 2(b) and (c), the addition of Ti element modified the structure and decreased the grain size compared with Fig. 2(a). A similar trend is also observed in the alloys containing Cr (Fig. 2(d)and (e)). SEM, EDS and XRD analysis of the various produced alloys are shown in Figs. 3 and 4. It was proved by EDS, atomic ratio in Fig. 3(a) and XRD analysis of alloy 1 that its microstructure mainly consists of primary α-Mg dendrite grains (spot 1) with eutectic phases (Al-riched α-Mg (spot 2) + β-$Mg_{17}Al_{12}$ (spot 3)) surrounding their boundaries. Fig. 3(b) and (d) shows that Ti and Cr addition affected the morphology and distribution of the β-$Mg_{17}Al_{12}$, respectively. In the case of Ti, eutectic morphology was changed to partially divorced eutectic, and the β-$Mg_{17}Al_{12}$ phase was transformed from network to globular form. Otherwise, the addition of Cr changed the eutectic morphology to partially divorced eutectic without changing the shape of the β-$Mg_{17}Al_{12}$ phase. The EDS map-

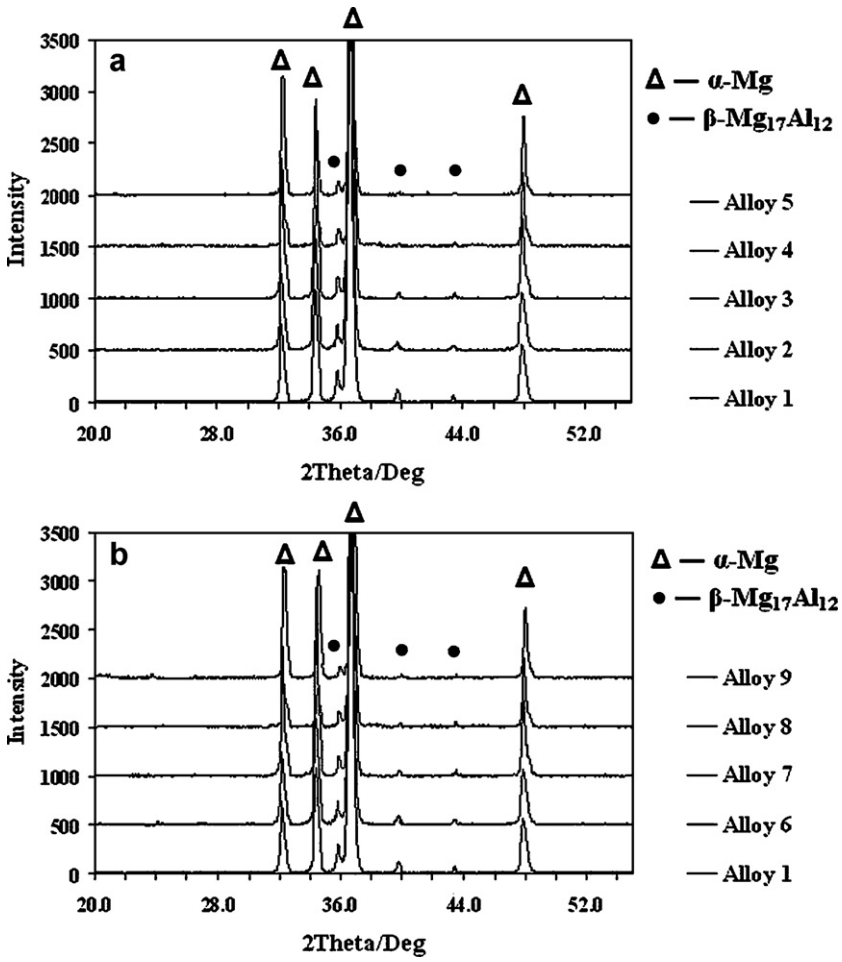

Fig. 4. The XRD spectrums of (a) alloy 1, 2, 3, 4, 5 and (b) alloy 6, 7, 8, 9.

ping of Alloy 5 in Fig. 3(c) shows that Ti has extremely low or unknown solubility in Mg lattice, and it is likely that fine particles of pure Ti exist at grain boundaries. Similar results were reported by Buha [18]. For the β-$Mg_{17}Al_{12}$ phase in Mg–6Al–*x*Ti alloys, titanium-containing particles may act as the heterogeneous nucleation site. Therefore, the one of the main effects of Ti on microstructure is the formation of partially divorced $Mg_{17}Al_{12}$ phase, as shown in Fig. 3(b). Similar results can be seen in Fig. 3(e) for Cr-containing Mg–Al alloy. As shown in Fig. 3(e), Cr, like Ti, has low or unknown solubility and exists at grain boundaries.

The XRD spectrums (Fig. 4(a) and (b)) of all the alloys show that Ti and Cr addition did not result in the formation of Ti or Cr containing any new phase. However, it can be seen in Fig. 4 that β-$Mg_{17}Al_{12}$ was detected in all specimens and the amount of β-phase was greatly reduced with increasing Ti and Cr.

The results of hardness, ultimate tensile, elongation and impact strength measurements of the specimen are given in Table 2. The hardness value of Ti-containing alloys up to 0.2 wt% increases with increasing alloying element concentration, and the hardness of alloy 1 is improved by 17%. Then the hardness is relatively constant with more addition of Ti. The hardness value of Cr containing alloys up to 0.2 wt% increased with increasing alloying element, and the hardness of alloy 1 was improved by 30% due to the addition of 0.2 wt% Cr. Then the hardness keeps on stable with more addition of Cr. As mention above, no information was found concerning Cr-containing Mg–Al alloys. The main parameters affecting the hardness are the solubility of the alloying element, grain size and eutectic morphology. The reason for the hardness increment can be attributed to smaller grain size, insolubility of Ti and Cr elements and homogeneous distributed eutectic areas.

The ultimate tensile strength (UTS) of alloy 1 is remarkably increased by Ti up to 0.2 wt% and is improved by 21%. Then the UTS is relatively constant with increasing Ti. A similar trend is also observed in the alloys containing Cr, and is improved by 15% due to the addition of 0.2 wt% Cr. The presence of brittle β-$Mg_{17}Al_{12}$ phase detrimentally influences the mechanical properties of Mg–Al alloys [12]. It is thought that UTS is affected by the change of the grain size and divorced eutectic structure. The reason that the UTS increased up to Ti and Cr 0.2 wt% was attributed to smaller grain size, the insolubility of Ti and Cr elements and the homogeneously

Table 2
Hardness, ultimate tensile strength, elongation and impact strength of the tested material.

	Hardness (HBN)	UTS (MPa)	Elongation at fracture (%e)	Impact strength (J)
Alloy 1	40(±1)	144(±10)	3,7(±0)	14(±0)
Alloy 2	46(±0)	162(±4)	6(±0,5)	16(±1)
Alloy 3	47(±1)	174(±6)	6,4(±0,5)	19(±2)
Alloy 4	47(±0)	172(±2)	6,4(±0,4)	18(±0)
Alloy 5	46(±0)	173(±2)	6,5(±0)	17.5(±1)
Alloy 6	47(±1)	155(±5)	5,5(±0,4)	15.5(±0)
Alloy 7	52(±2)	165(±6)	5,9(±0,5)	18(±1)
Alloy 8	51(±1)	164(±4)	5,8(±0)	17(±1)
Alloy 9	51(±1)	163(±5)	5,8(±0,4)	17(±0)

distributed eutectic areas. It is known that, the $Mg_{17}Al_{12}$ phase is incompatible with the magnesium matrix, which results in an incoherent and fragile $Mg/Mg_{17}Al_{12}$ interface [24]. The incoherence of the $Mg/Mg_{17}Al_{12}$ interface of alloy 1 was decreased due to the network of brittle β-$Mg_{17}Al_{12}$ phase in the alloy 1 destroys with addition of alloying elements. Hence, the elongation at fracture increment can be attributed to divorced eutectic morphology. In another view of the Table 2, the UTS and elongation at fracture

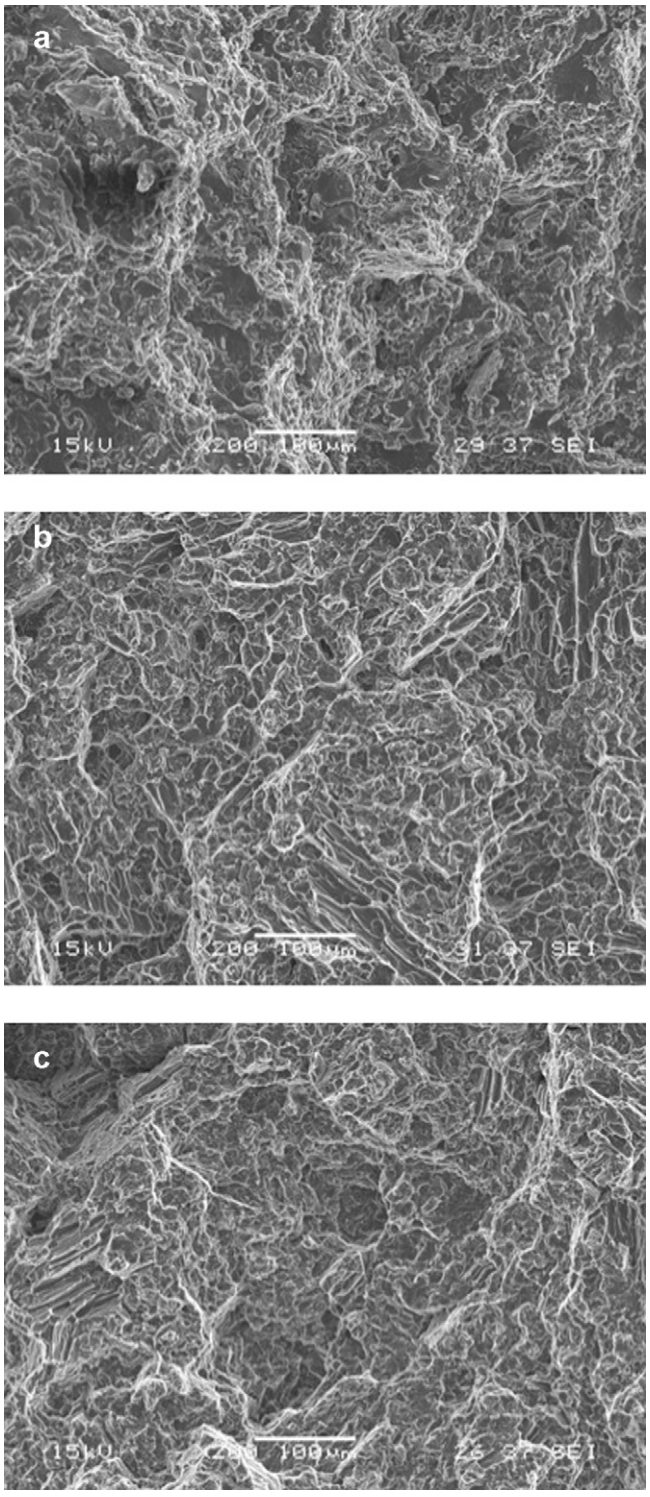

Fig. 5. SEM fractographs showing the morphology of fractured surfaces: (a) Mg–6Al, (b) Mg–6Al–0.2Ti, (c) Mg–6Al–0.2Cr alloy.

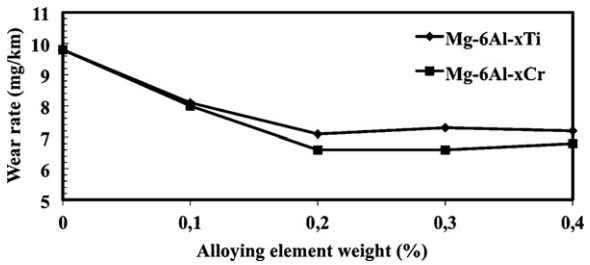

Fig. 6. Effect of alloying elements on the wear rate of the Mg–6Al alloy.

of the alloys with Ti are higher than those of the Cr alloys. In this study, Ti-containing alloys include globular β-$Mg_{17}Al_{12}$ phase in the grain boundaries, which can cause less stress concentration than Cr-containing alloys. Therefore, the ultimate tensile strength and elongation at fracture of the alloys containing Ti was higher than those of the Cr-containing alloys.

The impact strength value of alloy 1 was found 14 J. The result was in accordance with literature. Similar finding was reported by Schwam et al. [3]. As can be seen at Table 2, the impact strength of alloy 1 at room temperature is remarkably increased by Ti up to 0.2 wt%. The impact strength of alloy 1 was improved by 35% (from 14 J to 19 J) due to the addition of 0.2 wt% Ti. Then the impact strength is relatively constant with increasing Ti but remained the higher than the base alloy. A similar trend is also observed in the alloys containing Cr, and the impact strength of alloy 1 was improved by 28%(from 14 J to 18 J) due to the addition of 0.2 wt% Cr. In another view of the Table 2, the impact strength of the alloys with Ti is a little higher than those of the Cr alloys.

Examination of fracture surface of impact specimens via SEM manifests the fracture behavior of the alloys, which is shown in Fig. 5. The alloy with Ti and Cr exhibited different surface morphology compared to the base alloy Mg–6Al. While it was seen the large, wide fracture areas on the alloy 1 (Fig. 5(a)), some rod-like morphology and small, narrow fracture areas were observed in Fig. 5(b) and (c).

In this study, the addition of both alloying elements changed the microstructure of alloy 1. Hence, the increasing of impact strength of the alloys can be attributed to the microstructure. As shown before, the alloying elements decreased the size of the primary α-Mg dendrite grains and provided the formation of the partially divorced eutectic of $Mg_{17}Al_{12}$. Both the decreases in the grain size and the destroyed of the network of hard and brittle $Mg_{17}Al_{12}$ acted an important role in the increase on the impact resistance of the alloys. Furthermore, the formation of the divorced eutectic of $Mg_{17}Al_{12}$ let the primary α-Mg dendrite grains to come near to each other (there is no generally hard and brittle $Mg_{17}Al_{12}$ between primary α-Mg dendrite grains) then increased on the impact resistance. The impact resistance of the alloy is relatively constant with increasing alloying elements.

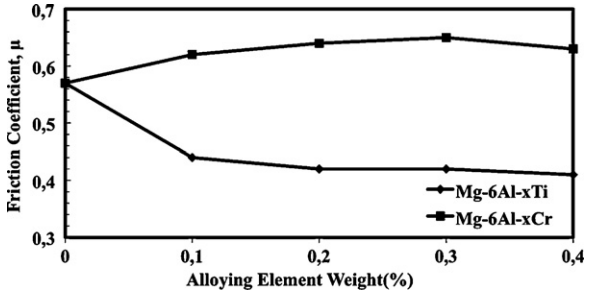

Fig. 7. Effect of alloying elements on the friction coefficient of the Mg–6Al alloy.

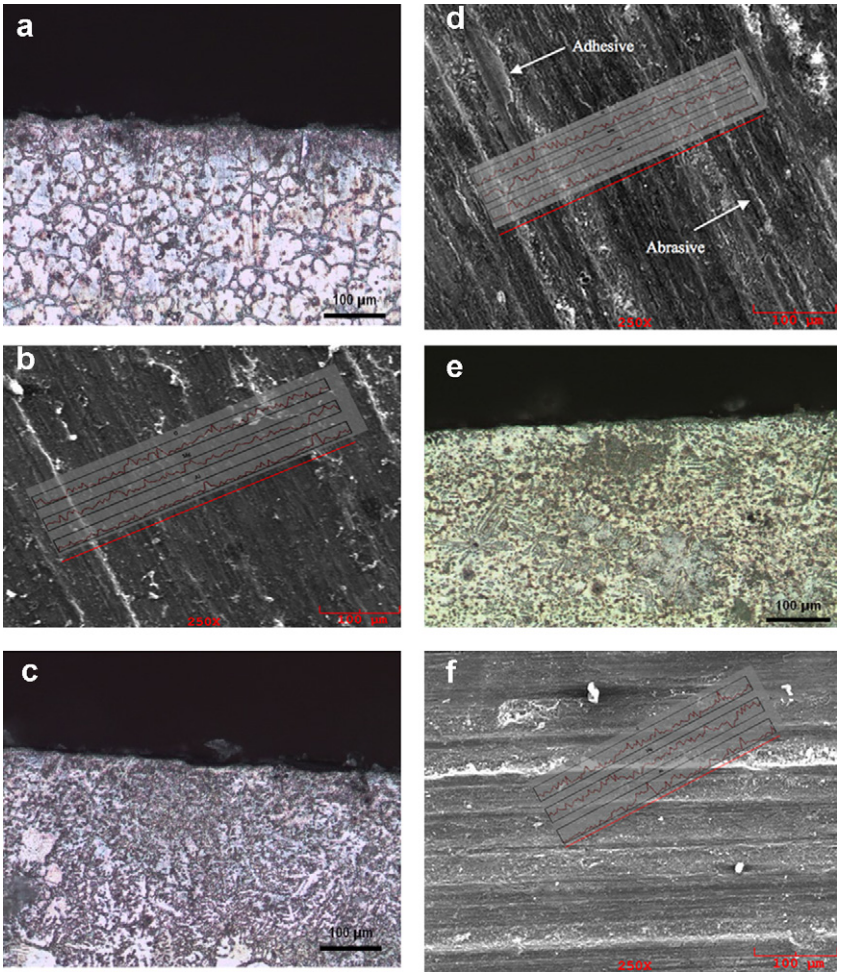

Fig. 8. Worn surface microstructure of: (a) and (b) Mg–6Al, (c) and (d) Mg–6Al–0.2Ti, (e) and (f) Mg–6Al–0.2 Cr alloy.

The effect of both alloying elements on the average wear rate and the friction coefficient is plotted in Figs. 6 and 7, respectively, as a function of alloying element. The wear rate of alloy 1 remarkably decreased with increasing Cr up to 0.2 wt%. Then the wear rate was relatively constant with the addition of more Cr. A similar trend is also observed in the alloys containing Ti (Fig. 6). It can be seen that the friction coefficient value of alloy 1 gradually increased with increasing Cr. However, the friction coefficient value of alloy 1 decreased with increasing Ti up to 0.2 wt%. Then the friction coefficient value is constant with increasing Ti, see Fig. 7.

Fig. 8 shows the wear tracks of alloys obtained under SEM and EDS analyses and OM results for the cross-section of the worn surface for dry sliding conditions. SEM analyses showed that both abrasive and adhesion wear mechanism observed on the worn surface of the alloys. As can be seen in OM results (Fig. 8(a), (c) and (e)), plastic deformation on the wear surface of the alloys was not observed and wear mechanism of the alloys was not changed with addition of alloying elements. Furthermore, EDS analyses reveals the formation of the oxide layer by indicating the presence of O, Mg and Al elements. The abrasive wear resulted in surface deformation and damage in the form of deep grooves in the sliding direction and the adhesion resulted plastering on the surface due to disparity of hardness between pin and steel disc, as shown obviously in Fig. 8(b), (d) and (f). As shown from Fig. 6 that the wear rate decreased up to 0.2 wt% alloying elements and it was not changed and approximately constant at higher content. The decrease on wear rate was attributed to the microstructure change and the hardness of the alloys. The alloying of Mg–6Al with Ti and Cr affected the microstructure of base alloy that is shown in Fig. 2. It was assumed that the formation of the partly divorced eutectic of $Mg_{17}Al_{12}$ was the main factor for decreasing the wear rate. As seen before, alloy 1 mainly contains continuous and brittle β-$Mg_{17}Al_{12}$. During the wear of the alloy 1, it is easily removed from the surface then behaved abrasive wear debris at the interface thereby the wear rate of the alloy 1 increased. However, the other alloys have small and modified β-$Mg_{17}Al_{12}$ so they showed resistance to wear. Furthermore, as a mentioned above that the wear rate is strongly dependent on the hardness of alloys. In this study, the hardness value of the base alloy increased with addition of the alloying elements.

4. Conclusions

(1) The addition of alloying elements has a pronounced grain-refining effect of Mg–6Al alloy.
(2) Metallographic studies showed that the addition of Ti and Cr elements changed the microstructure of Mg–6Al alloy and resulted in a partially divorced eutectic. The addition of alloying elements did not result in the formation of Ti or Cr containing any new phase.
(3) The hardness value of the alloys increased with both alloying elements content up to 0.2 wt%. Cr addition was much more effective than Ti on the hardness.
(4) Cr and Ti addition up to 0.2 wt% increased the UTS value of the alloys; the latter was much more effective than the former.

(5) Impact test studies showed that the addition of Ti and Cr alloying elements up to 0.2 wt% improved the impact strength of Mg–6Al alloy.
(6) The wear rate of Mg–6Al alloy remarkably decreased with increasing both alloying elements up to 0.2 wt%. Then the wear rate was relatively constant with the addition of more alloying elements. The friction coefficient value of Mg–6Al alloy gradually increased with increasing Cr. However, the friction coefficient value of Mg–6Al alloy decreased with increasing Ti up to 0.2 wt%.

Acknowledgement

The authors would like to thank the Scientific and Technical Research Council of Turkey-TÜBİTAK for financial support in this research.

References

[1] A. Yu, S. Wang, N. Li, H. Hu, Pressurized solidification of magnesium alloy AM50A, J. Mater. Process. Technol. 191 (2007) 247–250.
[2] H. Hu, Squeeze casting of magnesium alloys and their composites, J. Mater. Sci. 33 (1998) 1579–1589.
[3] D. Schwam, J. Wallace, Y. Zhu, S. Viswanathan, S. Iskender, Enhancements in Magnesium Die Casting Impact Properties-Final Report, Case Western Reserve University, Ohio, 2000.
[4] H.Q. Sun, Y.N. Shi, M.X. Zhang, Wear behavior of AZ91D magnesium alloy with a nanocrystalline surface layer, Surf. Coat. Technol. 202 (2008) 2859–2864.
[5] W. Huang, B. Hou, Y. Pang, Z. Zhou, Fretting wear behavior of AZ91S and AM60B magnesium alloys, Wear 260 (2006) 1173–1178.
[6] D.S. Mehta, S.H. Masood, W.Q. Song, Investigation of wear properties of magnesium and aluminum alloys for automotive applications, J. Mater. Process. Technol. 155–156 (2004) 1526–1531.
[7] H. Chen, A.T. Alpas, Sliding wear map for the magnesium alloy Mg–9Al–0.9 Zn (AZ91), Wear 246 (2000) 106–116.
[8] M. Shanthi, C.Y.H. Lim, L. Lu, Effects of grain on the wear of recycled AZ91 Mg, Tribol. Int. 40 (2007) 335–338.
[9] M. Zhou, H. Hu, N. Li, J. Lo, Microstructure and tensile properties of squeeze cast magnesium alloy AM50, J. Mater. Eng. Perform. 14 (2005) 539–545.
[10] A.K. Dahle, Y.C. Lee, M. Nave, P. Schaffer, D. StJohn, Development of the as-cast microstructure in magnesium–aluminum alloys, J. Light Met. 1 (2001) 61–72.
[11] T.A. Leil, N. Hort, W. Dietzel, C. Blawert, Y. Huang, K.U. Kainer, K.P. Rao, Microstructure and corrosion behavior of Mg–Sn–Ca alloys after extrution, Trans. Nonferrous Met. Soc. China 19 (2009) 40–44.
[12] S. Kleiner, O. Beffort, A. Wahlen, P.J. Uggowitzer, Microstructure and mechanical properties of squeeze casting and semi-solid cast of Mg–Al alloys, J. Light Met. 2 (2002) 277–280.
[13] Y.V.R.K. Prasad, K.P. Rao, N. Hort, K.U. Kainer, Optimum parameters and rate-controlling mechanisms for hot working of extruded Mg–3Sn–1Ca alloy, Mater. Sci. Eng. A 502 (2009) 25–31.
[14] S. Li, B. Tang, D. Zeng, Effects and mechanism of Ca on refinement of AZ91D alloy, J. Alloys Compd. 437 (2007) 317–332.
[15] S. Cohen, G.R. Goren-Mugistein, S. Avraham, G. Dehm, M. Bamberger, in: H.A. Luo (Ed.), Magnesium Technology, TMS, USA, 2004, pp. 301–305.
[16] N. Hort, Y. Huang, K.U. Kainer, Intermetallics in magnesium alloys, Adv. Eng. Mater. 8 (2006) 235–240.
[17] Y.C. Lee, A.K. Dahle, D.H. StJohn, The role of solute in grain refinement of magnesium, Metall. Mater. Trans. A 31A (2000) 2895–2906.
[18] J. Buha, Natural ageing in magnesium alloys and alloying with Ti, J. Mater. Sci. 43 (2008) 1220–1227.
[19] P. Zhao, Q. Wang, C. Zhai, Y. Zhu, Effects of strontium and titanium on the microstructure, tensile properties and creep behavior of AM50 alloys, Mater. Sci. Eng. A 444 (2007) 318–326.
[20] P. Bala Srinivasan, C. Blawert, W. Dietzel, Dry sliding wear behavior of a conventional and recycled high pressure die cast magnesium alloys, Mater. Charact. 60 (2009) 843–847.
[21] M.X. Liang, W. Xiang, L.X. Lin, Y. Lei, Effect of Al5Ti1B master alloy on microstructures and properties of AZ61 alloys, Trans. Nonferrous Met. Soc. China 20 (2010) 397–401.
[22] T.R. Ramachandran, P.K. Sharma, K. Balasubramanian, Grain Refinement of Light Alloys, World Foundry Congress, 2008, pp. 189–193.
[23] D. Qiu, M.X. Zhang, Effect of active heterogeneous nucleation particles on the grain refining efficiency in an Mg–10 wt%Y cast alloy, J. Alloys Compd. 488 (2009) 260–264.
[24] Y.Z. Lu, Q.D. Wang, W.J. Ding, X.Q. Zeng, Y.P. Zhu, Fracture behavior of AZ91 magnesium alloy, Mater. Lett. 44 (2000) 265–268.